ChemPubSoc Europe

DOI: 10.1002/chem.201403737

CHEMISTRY
A European Journal
Full Paper

Rearrangements

Evaluating the Thermal Vinylcyclopropane Rearrangement (VCPR) as a Practical Method for the Synthesis of Difluorinated Cyclopentenes: Experimental and Computational Studies of Rearrangement Stereospecificity

David Orr,[a] Jonathan M. Percy,*[a] Tell Tuttle,[a] Alan R. Kennedy,[a] and Zoë A. Harrison[a, b]

Abstract: Vinyl cyclopropane rearrangement (VCPR) has been utilised to synthesise a difluorinated cyclopentene stereospecifically and under mild thermal conditions. Difluorocyclopropanation chemistry afforded ethyl 3-(1′(2′2′-difluoro-3′-phenyl)cyclopropyl) propenoate as all four stereoisomers (**18a**, **18b**, **22a**, **22b**) (all racemic). The *trans-E* isomer (**18a**), prepared in 70% yield over three steps, underwent near quantitative VCPR to difluorocyclopentene **23** (99%). Rearrangements were monitored by ^{19}F NMR (100–180 °C). While *cis*/*trans* cyclopropane stereoisomerisation was facile, favouring *trans*-isomers by a modest margin, no *E*/*Z* alkene isomerisation was observed even at higher temperatures. Neither *cis* nor *trans Z*-alkenoates underwent VCPR, even up to much higher temperatures (180 °C). The *cis*-cyclopropanes underwent [3,3]-rearrangement to afford benzocycloheptadiene species. The reaction stereospecificity was explored by using electronic structure calculations, and UB3LYP/6-31G* methodology allowed the energy barriers for cyclopropane stereoisomerisation, diastereoisomeric VCPR and [3,3]-rearrangement to be ranked in agreement with experiment.

Introduction

The rearrangement of vinylcyclopropanes to cyclopentenes (the vinylcyclopropane rearrangement, VCPR) has developed rapidly from its initial discovery by Neureiter over 70 years ago,[1] becoming an important transformation in the synthesis of a variety of complex natural products.[2] The synthetic scope of the reaction has expanded significantly;[3,4] while the prototypical reaction of **1** to **2** required high temperatures for the rearrangement of the simple parent hydrocarbon[5,6] (Scheme 1), substrate modifications[7] and the deployment of transition metal catalysts[8–10] have even allowed the rearrangement to be carried out at room temperature in some cases.

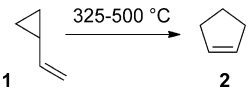

Scheme 1. Prototypical vinylcyclopropane rearrangement (VCPR).

Rearrangements which can be carried out at lower temperature are desirable because they minimise the risk of competing and unwanted stereoisomerisation[11,12] and homodienyl [1,5]-hydrogen shifts.[13]

The activation energy for the prototypical VCPR was independently reported by Wellington[14] ((50 ± 0.3) kcal mol^{-1}) and Baldwin[15] ((51.7 ± 0.5) kcal mol^{-1}) to be approximately 13 kcal mol^{-1} less than the energy required to break a cyclopropane C–C bond.[16] The similarity of that quantity to the resonance stabilisation energy of the allyl radical (calculated as (12.4 ± 0.6) kcal mol^{-1} [17]) supports the idea that the rearrangement proceeds via diradical intermediates strongly. Difluorinated **3**[18,19] and perfluorinated **4a**[20] precursors (Figure 1) have lower

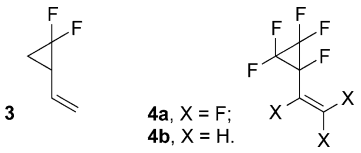

Figure 1. Fluorinated VCPR precursors from the literature.

activation energies by up to 10.3 and 17.1 kcal mol^{-1}, respectively. More recently, Smart and co-workers reported that pentafluorinated **4b** underwent facile rearrangement, with the lowest reported activation energy of 28.4 kcal mol^{-1} (23.3 kcal mol^{-1} less than the prototypical VCPR).[21] This was attributed to the higher strain energy of fluorinated cyclopropanes. O'Neal and Benson[22] proposed that the strain energy increas-

[a] D. Orr, Prof. Dr. J. M. Percy, Dr. T. Tuttle, Dr. A. R. Kennedy, Dr. Z. A. Harrison
WestCHEM Department of Pure and Applied Chemistry
University of Strathclyde, Thomas Graham Building
295 Cathedral Street, Glasgow G1 1XL (UK)
Fax: (+44) 141-548-4822
E-mail: jonathan.percy@strath.ac.uk

[b] Dr. Z. A. Harrison
Refractory Respiratory Inflammation DPU
GlaxoSmithKline Medicines Research Centre, Gunnels Wood Road
Stevenage, SG1 2NY (UK)

Supporting information for this article is available on the WWW under http://dx.doi.org/10.1002/chem.201403737.

es by approximately 5 kcal mol^{-1} per fluorine atom; this idea was later supported by experimental[19] and computational work.[23] Extensive studies by Dolbier and co-workers[24,25] showed that *gem*-difluorinated cyclopropanes undergo regiospecific ring opening via cleavage of the weaker distal carbon–carbon bond.

Despite these seminal and fundamental studies of reactivity, the VCPR has not been deployed as a method for the synthesis of difluorinated cyclopentenes. Because of Dolbier's recent significant progress in difluorocyclopropanation methodology,[26] we sought to develop a building block approach[27] to difluorinated cyclopentenes based on the VCPR, which would exploit fluorine atom effects to decrease the reaction temperatures of the simple thermal rearrangements.

The proposed strategy was based on the synthesis of difluorinated analogue **8** of a dictyopterene pheromone found in brown algae, reported by Boland and Erbes[28] (Scheme 2).

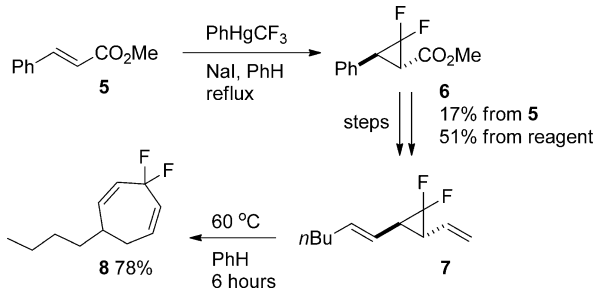

Scheme 2. Boland and Erbes' synthesis of Dictyopterene analogue **8**.

The conversion of alkenoate **5** to cyclopropane **6** required the use of Seyferth's reagent ($PhHgCF_3$), the most reactive difluorocarbene transfer reagent available. The reaction was sacrificial in **5**, and the yield of cyclopropanation was only moderate (51% based on the reagent). Seyferth's reagent is highly toxic and is not readily available, limiting its utility considerably. With the alkenyl groups in place, the diyl rearrangement of **7** to **8** was efficient and facile.

Difluorocyclopropanation of *E*-cinnamyl acetate **9**, then ester hydrolysis to **11**, followed by tandem oxidation/olefination would secure VCPR precursor **12** via a simple and direct sequence (Scheme 3), setting the stage for rearrangement to **13**.

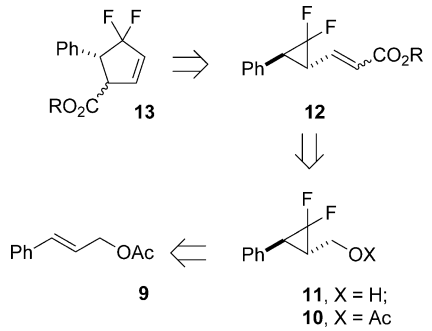

Scheme 3. Proposed route to difluorinated cyclopentene 13.

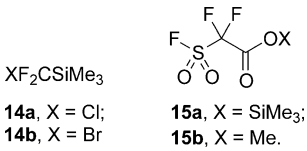

14a, X = Cl; **14b**, X = Br

15a, X = $SiMe_3$; **15b**, X = Me.

Figure 2. Selected reagents used for difluorocyclopropanation.

One prerequisite for a successful route would be a highly efficient difluorocyclopropanation of **9**.

A very wide range of difluorocyclopropanation reagents is now available (Figure 2).[29–31] Inexpensive sodium chlorodifluoroacetate has been used to transform relatively electron-deficient substrates like **9** but significant excesses of the reagent are usually required.[32–34]

Seyferth's reagent[35,36] was unacceptable, so we sought more recent methods. Hu et al.[37] used (chlorodifluoromethyl)-trimethylsilane **14a** (prepared from bromochlorodifluoromethane[38]) as a difluorocarbene precursor, securing difluorocyclopropanes from a range of alkenes and alkynes. More recently the same group reported that a more general reagent, (bromodifluoromethyl)trimethylsilane **14b**, could not only effect cyclopropanation but also difluoromethylate oxygen, sulfur, nitrogen and phosphorus nucleophiles.[39] While the reagent was effective in many cases, the yield of cyclopropane obtained from benzyl acrylate was only moderate (43%).

The current benchmark reagent, trimethylsilyl fluorosulfonyldifluoroacetate (TFDA) **15a** was reported by Dolbier and coworkers in 2000.[40] Fluoride-catalysed decomposition of **15a** in the presence of alkenes results in efficient cyclopropanation; for example, the reaction with benzyl acrylate afforded the cyclopropane in 73% yield. More recently, the Gainesville group reported that the more robust methyl 2,2-difluoro-2-(fluorosulfonyl)acetate (MDFA) **15b** would effect many of the TFDA reactions successfully.[26] These reagents looked like extremely promising starting points for our study.

Results and Discussion

Following disappointing results with a range of carbene precursors (see the Supporting Information for details), carbene formation and trapping was attempted with **9** and MDFA **15b** under the conditions described by Dolbier. We failed to achieve full conversion of alkene **9** and isolated a previously unobserved side product (Table 1, entry 1). The presence of iodide in the reaction mixture could result in (S_N2') nucleophilic ring opening with strain relief to afford iodide **16**; this side product could be isolated successfully from the crude reaction mixture using column chromatography, but the yellow/brown oil decomposed after storage in the refrigerator (see the Supporting Information for the ^1H and ^{19}F NMR spectra which support the assignment). A 0.25-fold increase in reagent excess over alkene **9** increased the conversion to 95% after 17 h (Table 1, entry 2). The Dolbier group experienced similar problems during their optimisation, reporting that reducing the reaction concentration led to poorer yields.

Table 1. Optimisation with MDFA **15b**.

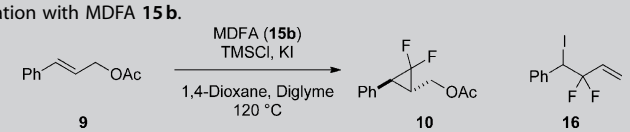

9 **10** **16**

Entry	**15b** [equiv]	TMSCl [equiv]	Dioxane [equiv]	Diglyme [equiv]	KI [equiv]	Time [h]	Conversion (9:10)[a]	Yield [%][b]
1	2	2	1.7	0.1	2.25	48	4:80[c]	32
2	2.46	2.46	1.87	0.11	2.77	17	1:19	43
3	2.46	2.46	0	1.2[d]	2.77	24	0:1	94
4	2.46	2.46	0	1.2	2.77	4	0:1	85

[a] Determined by crude ^{1}H NMR spectroscopy. [b] Isolated yield. [c] Crude reaction mixture contained 16% **16** (^{1}H NMR spectroscopy). [d] Reaction mixture went to dryness after 5 h and an extra 1.2 equiv of diglyme was added.

The reaction in diglyme alone afforded **10** in high yield (94%; Table 1, entry 3) if an additional portion of diglyme was added when the reaction mixture started to solidify. When the reaction was stopped after only 4 h, full conversion was achieved and the high yield of **10** was maintained (85%; Table 1, entry 4).

Ester **10** was saponified to afford alcohol **11** in high yield (Scheme 4). Gram quantities of material could be brought through (8 mmol scale from **9**), giving access to synthetically useful quantities of alcohol **11** over two steps. Vatéle's one-pot oxidation/olefination conditions[41] were implemented next because they avoided isolation of potentially fragile aldehyde **17**. Oxidation of **11** by a TEMPO–BAIB combination, gave full conversion to aldehyde **17** after 6 h (the reaction was monitored by ^{19}F NMR spectroscopy). Addition of (carbethoxymethylene)triphenylphosphorane afforded a separable mixture of **18a** and **18b** (95:5 by ^{1}HNMR spectroscopy).

The *cis*-precursors were prepared from **19**, via Lindlar reduction and acetylation (86% over 2 steps); elaboration as before afforded **22a** (71%) and **22b** (17%) after the oxidation/olefination step. Cyclopropane and alkene relative configuration was confirmed by NOESY and ^{1}H NMR spectroscopy, respectively, for all four products (see the Supporting Information).

We found that **18a** rearranged smoothly to difluorocyclopentene **23** even at 90 °C (Table 2, entry 1). Cyclopropane stereoisomerisation was also observed (by ^{19}F NMR spectroscopy after 6 h); the *cis* diastereoisomer **22a** was formed from pure *trans*-**18a**, but thermolysis of the **18a**/**22a** mixture resulted in the formation of unique difluorocyclopentene product **23**. The product connectivity was established by 2D NMR spectroscopy (HSQC/HMBC) and the *trans*-configuration was assigned from ^{1}H/^{1}H and ^{1}H/^{19}F NMR coupling constant analysis (see the Supporting Information for details). The assignment was confirmed when **23** was oxidised to crystalline epoxide **24** (Scheme 5) using methyl(trifluoromethyl)dioxirane prepared according to a modification of a published procedure[42] described by the Baran group.[43] The original *trans*-relationship and the unexpected facial selectivity (vide infra) were shown by the elucidation of the molecular structure in the crystal (see the Supporting Information for more details and a discussion).

Microwave irradiation resulted in slower rearrangement (Table 2, entry 2), but neat **18a** was consumed more rapidly under conventional heating ((Table 2, entry 3). Under these conditions, side product **25a** was also formed. [3,3]-Rearrangement[44] of *cis*-cyclopropane **22a**,

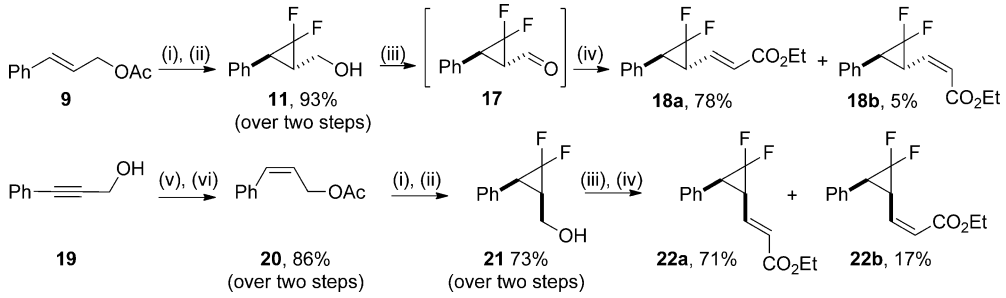

Scheme 4. Synthesis of VCPR precursors **18** and **22**. Conditions: i) MDFA (2.46 equiv), TMSCl (2.46 equiv), KI (2.77 equiv), diglyme (1.2 equiv), 120 °C, 24 h; ii) K_2CO_3 (1 equiv), MeOH/H_2O, 60 °C, 2 h; iii) TEMPO (2,2,6,6-tetramethylpiperidine 1-oxyl, 0.1 equiv), BAIB ($PhI(OAc)_2$, 1.15 equiv), DCM, r.t., 6 h; iv) $Ph_3P{=}CHCO_2Et$ (1.3 equiv) 2–14 h; v) H_2 (1 equiv, atm), Lindlar cat. (5 mol% Pd), EtOH, r.t., 10 h; vi) Ac_2O (1.05 equiv) DMAP (10 mol%), DCM/pyridine, r.t., 22 h.

Table 2. Selected optimisation results for thermal VCPR of **18a** and **22a**.

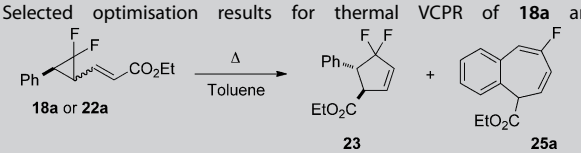

18a or **22a** **23** **25a**

Entry	VCP	Temp. [°C]	Time [h]	Conversion[a] **18a**	**22a**	**23**	**25a**	Yield [%][b]
1	**18a**	90	6	1	0.19	0.63	0	–
			26	1	0	4.6	0	
2[c]	**18a**	90	6	1	0.14	0.11	0	–
3[d]	**18a**	90	22	1	0	33	17	–[e]
4	**18a**	100	17	0	0	1	0	99
5	**22a**	100	24	0	0	1	0	93

[a] Ratio determined by ^{19}F NMR spectrscopy. [b] Isolated yield. [c] Microwave irradiation. [d] Neat reaction mixture. [e] Compound **25a** isolated in 19% yield.

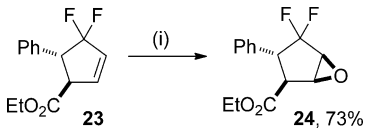

Scheme 5. Dioxirane oxidation of VCPR product **23**. Conditions: i) Methyl(trifluoromethyl)dioxirane (ca. 3.4 equiv) in trifluoroacetone, −78 °C, 1 h then r.t., 1 h.

followed by dehydrofluorination/rearomatisation of the initial precursor (vide infra) results in the formation of **25a**; the connectivity was established by 2D NMR methods (see the Supporting Information for details). The side reaction could be avoided when the reaction was run in toluene at 100 °C (Table 2, entry 4). Upon full conversion (determined by ^{19}F NMR spectroscopy) under these conditions, the reaction solvent was removed to afford a very high yield of **23** from **18a** (99%); **22a** also rearranged exclusively to **23** in excellent (93%) yield under the same conditions (Table 2, entry 5) (see the Supporting Information for examples of crude VCPR spectra). The relatively high reactivity of our precursor system is consistent with the presence of the CF_2 centre and the development of benzylic radical character; Ingold and co-workers[45] and Newcomb et al.[46,47] showed that cyclopropyl radical ring opening was accelerated strongly when the product radical was benzylic. Roth and co-workers showed that the VCPR of **3** only occurred above 200 °C[19] so the phenyl group is providing strong activation.

This VCPR represents a direct and effective way of making difluorinated cyclopentenes. Whereas radical cyclisation methods (based on tin hydride chemistry) were deployed by several groups to access difluorinated cyclopentanes,[48–50] diethylaminosulfur trifluoride (DAST) or DeoxoFluor ketone transformations have secured difluorinated cyclopentanones,[51] and Nazarov cyclisations[52] difluorinated cyclopentenones. Difluorinated cyclopentenes are relatively unusual motifs in the synthetic literature.[53] Qing and co-workers[54] used ring-closing metathesis (RCM) to form the key cyclopentene ring of carbanucleosides in which CF_2 replaces a furanyl ring oxygen, and Itoh has also used an RCM approach in which difluorocyclopropane ring-opening fulfils a pivotal role.[55] Our VCPR-based approach combines ease of preparation (four high-yielding steps from commercially available reagents) with an attractive range of functional groups for further transformation. Previously we have used difluorinated cycloalkenes as precursors to difluorinated carbasugar analogues,[56–58] and exploited the Sharpless oxidation of phenyl groups in syntheses of difluorinated aldoses.[59]

To investigate the role of cyclopropane stereoisomerisation more fully, the reactions of both **18a** and **22a** were monitored by ^{19}F NMR spectroscopy at 373 K in [D_8]toluene (see the Supporting Information for experimental details). As shown in Table 2, **18a** transformed smoothly to **23**, but **22a** also formed, reaching a maximum at about 13% of the reaction mixture after 10 min, and then decaying slowly, showing that cyclopropane stereoisomerisation (Figure 3a) competes effectively with VCPR. This was observed more clearly when the reaction was started from **22a**; within 15 min, most of the *cis*-cyclopropane had isomerised to the *trans*-diastereoisomer **18a**, which then reacted through to **23** (Figure 3b).

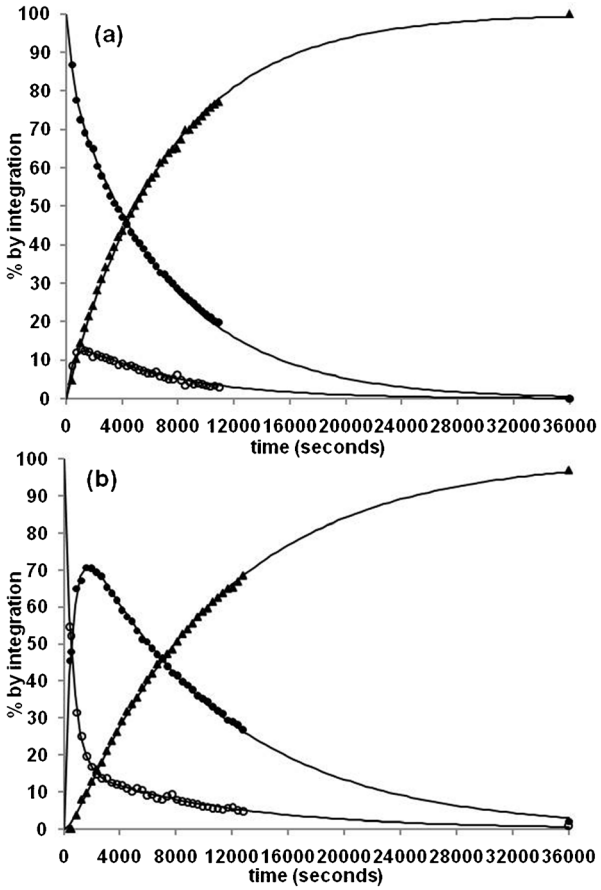

Figure 3. Experimental (points) and simulated (lines) concentration/time profile for thermolysis (373 K) of a) **18a**; b) **22a**; **18a** = ●, **22a** = ○, **23** = ▲).

The concentration/time profiles could be simulated successfully as far as experimental endpoints at 10 h using numerical integration software (see the Supporting Information for details) based on the simple model of Scheme 6.

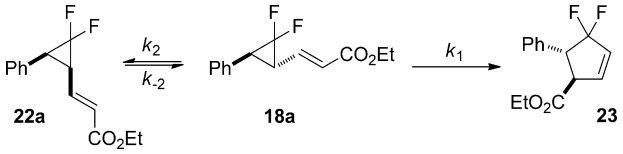

Scheme 6. Kinetic model used in the simulation of parallel VCPR and stereoisomerisation pathways.

Deconvolution of the rate constants (Table 3) highlighted the modest equilibrium constant between *trans* and *cis* cyclopropanes (5.4 starting from *trans*, 5.6 starting from *cis*, in favour of the *trans*-diastereoisomer) and the facile stereoisomerisation (the rate constant is an order of magnitude higher than that for VCPR).

An approximate Arrhenius determination of activation parameters was carried out by taking the best first-order fit of

Table 3. Rate constants extracted from reaction simulation.

Substrate	$10^4\ k_1\ [s^{-1}]$	$10^4\ k_2\ [s^{-1}]$	$10^4\ k_{-2}\ [s^{-1}]$	k_{-2}/k_2
18a	1.6	3.5	19.1	5.4
22a	1.1	2.6	14.7	5.6

the data from VCPR of **18a** from NMR experiments (363-393 K, [D_8]toluene) (see the Supporting Information for experimental details); a value for E_a of (29.2 ± 0.6) kcal mol^{-1}, not unlike that obtained by Smart and co-workers (28.4 kcal mol^{-1} at 373 K) for thermolysis of **4b**.

We failed entirely to detect VCPR from either *Z* species (**18b** or **22b**) (Figure 4); only stereoisomerisation was detectable

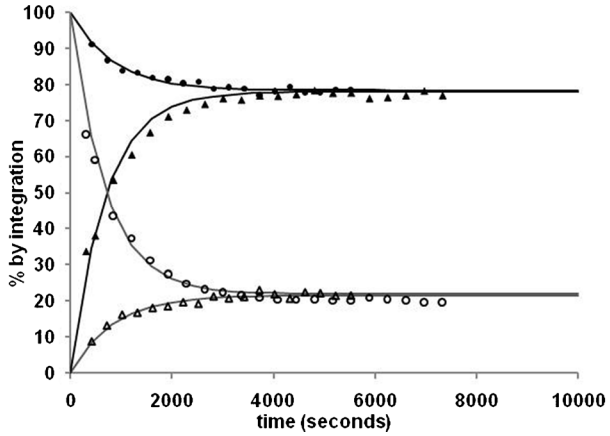

Figure 4. Experimental (points) and simulated (lines) concentration/time profile for thermolysis of **18b** and **22b** (starting from: ● **18b** from **18b**; ▲ **18b** from **22b**; ○ **22b** from **22b**; Δ **22b** from **18b** ([D_8]toluene, 373 K)).

when either **18b** or **22b** was heated in [D_8]toluene at 373 K. Equilibrium constants of 3.7 (from **18b**) and 3.6 (from **22b**) favouring **18b** were extracted from the simulation data and confirmed by integration of the ^{19}F NMR spectra (see the Supporting Information).

At higher temperature (180 °C), **18b** underwent [3,3]-rearrangement to **25a** and **25b** (10:1 by ^{19}F NMR integration) (Scheme 7).

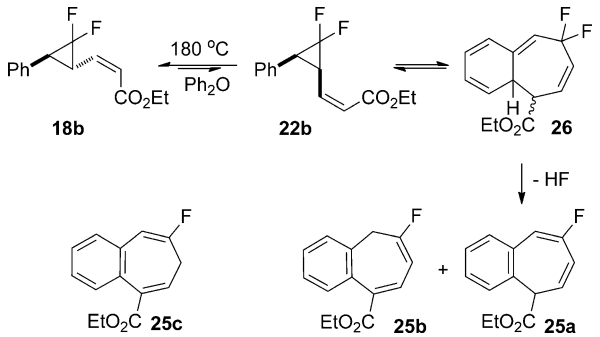

Scheme 7. [3,3]-Rearrangement of *Z*-alkenoate precursors **18b** and **22b**.

Stronger heating of **22b** also returned a very similar mixture of **25a** and **25b** (9:1 by ^{19}F NMR integration). De-aromatised intermediate **26** was never observed; elimination of HF driven by re-aromatisation would be anticipated strongly. Heating isolated **25a** to 180 °C (Ph_2O, 17.5 h) returned more fully conjugated **25b**, presumably via an [1,5]-H shift; **25c** (the product of [1,3]-H shift from **25a**) was not detected.

The inertness of the *Z*-alkenoate precursors towards VCPR surprised us, but we failed to find examples of *Z*-alkenyl groups participating, apart from the deuterated species of Baldwin and co-workers.[60,61] Sustmann[62] and co-workers prepared precursors with *Z*-alkenyl groups but did not report their behaviour under rearrangement conditions. Smart et al.[21] heated a 5:1 mixture of **27a** and **27b**, to form a 19:1 mixture of pentafluorocyclopentene **28** and unreacted *Z*-isomer **27b** (Scheme 8). To our knowledge, Smart's result provides the only

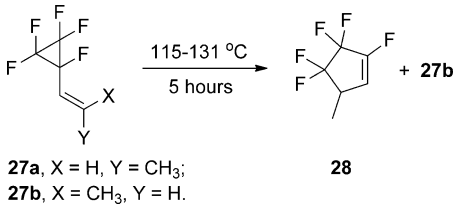

Scheme 8. Convergence of diastereoisomeric alkene precursors through VCPR.

example of a Z-alkenyl motif taking part in VCPR; $\Delta G^{\ddagger}$ (373 K) for the VCPR of **27b** was measured at 31.1 kcal mol^{-1}, only approximately 3 kcal mol^{-1} higher than that for **27a** (28.5 kcal mol^{-1}).

The *E*/*Z* reactivity difference is more dramatic in our system. This and other aspects of the reaction stereospecificity were now examined using electronic structure calculations.

Davidson and Gajewski,[63] and Houk and co-workers,[64,65] have used computational methods to study the vinylcyclopropane rearrangement. A detailed dynamics treatment has also been reported.[66] The parent system **1** undergoes VCPR and stereoisomerisation competitively but the major reaction channel involves VCPR via the Woodward–Hoffmann "allowed" suprafacial inversion (*si*) transition state **TS1** leading to cyclopentene **2** (Scheme 9).

In their seminal study,[65] Houk and co-workers reported that unrestricted B3LYP[67,68] (UB3LYP/6-31G*) predicted experimental VCPR activation energies well. However, more recent work[62] has proposed a combination of Truhlar's M05-2X hybrid functional[69–71] and the 6-311 + G** basis as a benchmarking method.

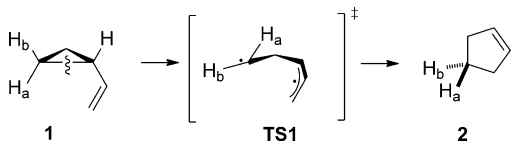

Scheme 9. VCPR *si*-transition state **TS1**, showing the exchange of the H_a and H_b ligands through inversion at the migratory carbon centre.

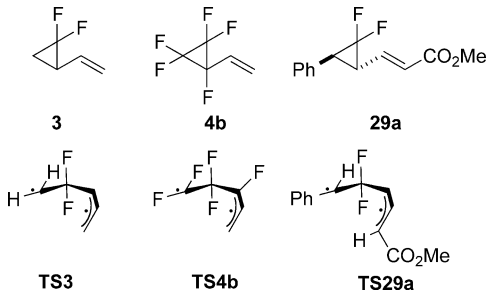

Figure 5. VCPR precursors and their corresponding transition states.

We chose to explore the effectiveness of a small matrix of methods for the prediction of VCPR barriers. We selected VCP/VCPR systems **1**, **3**, **4b** and **29a** (a conformationally simpler analogue of **18a**) (Figure 5), and used B3LYP, M05-2X, M06-2X[72] and B97-D[73,74] functionals (all in unrestricted mode) with 6-31G*, 6-31+G* and 6-311+G** basis sets to calculate barrier energies ($\Delta G^{\ddagger}$). Geometry optimisations were performed in Gaussian'09,[75] Spartan'08[76] or Spartan'10;[77] the optimised geometries were characterised as minima or transition structures by performing harmonic frequency calculations.

As the focus of our work is primarily synthetic, we wished to establish an effective method of lowest cost, so that we could use it for the design of new reaction systems which would undergo relatively facile rearrangement. In each case, the *s-trans Z* or *s-trans E* cyclopropane geometry and the transition structure on the suprafacial inversion (*si*) pathway were optimised with full frequency calculation. Because the dipoles of all the precursors and transition structures were small and similar (2.25–3.00 Debyes), and the toluene solvent used for the experimental work has a low dielectric constant ($\varepsilon = 2.38$), we have not applied solvation methods.

We used Houk's Cartesian coordinates[65] for **TS1** as a starting point for structure building and transition state searching; in the case of **TS29a**, a range of diastereoisomeric and conformationally isomeric species was explored (vide infra). Table 4 and Figure 6 compare the computational results to values of $\Delta G^{\ddagger}$ (298 K) calculated from experimental Arrhenius parameters (E_a, A) from the literature and from this work.

Table 4. Barriers ($\Delta G^{\ddagger}$, gas phase, 298 K, kcal mol^{-1}) for VCPR from electronic structure calculations (ESC) and recalculated[78] from Arrhenius data.[15,18,21]

Method	1→TS1	3→TS3	4b→TS4b	29a→TS29a
UB3LYP 6-31G*	46.9	38.3	24.8	26.6
UB3LYP 6-31+G*	46.2	36.0	22.9	25.1
UB3LYP 6-311+G**	45.9	36.0	23.0	24.8
UM05-2X 6-31G*	50.8	41.6	28.5	31.1
UM05-2X 6-31+G*	50.0	39.4	26.4	29.8
UM05-2X 6-311+G**	49.5	39.5	26.8	29.8
UM06-2X 6-31G*	55.1	46.4	31.8	36.0
UM06-2X 6-31+G*	54.0	44.0	29.9	34.7
UM06-2X 6-311+G**	53.2	43.6	29.8	34.6
UB97-D 6-31G*	45.3	36.2	29.7	22.5
UB97-D 6-31+G*	44.6	33.9	28.0	21.3
UB97-D 6-311+G**	44.4	36.8	27.9	21.1
experiment	49.2	39.0	28.5	28.6

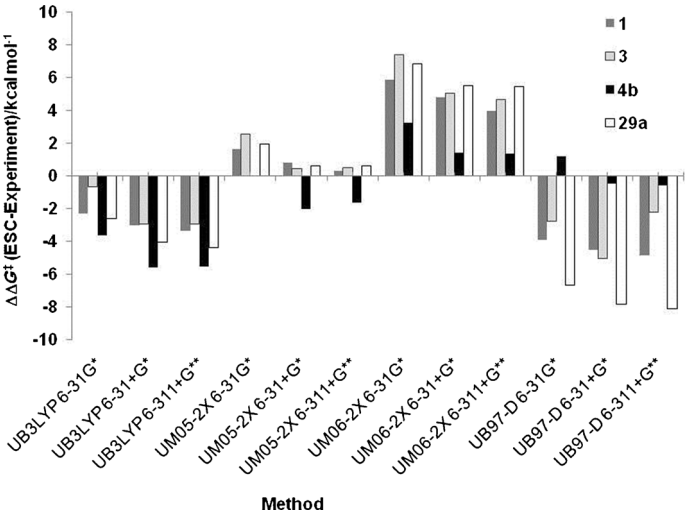

Figure 6. Differences between experimental $\Delta G^{\ddagger}$ (298 K, re-calculated from activation parameters) and $\Delta G^{\ddagger}$ from electronic structure calculations (298 K), plotted as $\Delta\Delta G^{\ddagger}$ ($\Delta G^{\ddagger}$(ESC)$-\Delta G^{\ddagger}$(experimental), kcal mol^{-1}). Expected error associated with data is ± 0.5 kcal mol^{-1}.

There were significant differences between the levels of performance of the functionals. UB3LYP underestimated the experimental barriers for all systems, with the discrepancy increasing with basis set size. UB97-D performed best with Smart's highly fluorinated system but under-estimated barriers for the other systems with all basis sets. The imaginary frequencies calculated for **TS4b** and **TS29a** with UB97-D were much lower than with the other functionals, and the values of the spin operator $<S^2>$ were 0 for **4b** and 0.251–0.311 for **TS29a**, whereas consistently higher values were obtained with the other methods for all systems (see the Supporting Information for details).

The closest agreement with experimental values was obtained with UM05-2X/6-31+G* and UM05-2X/6-311+G** methods with $\Delta\Delta G^{\ddagger}$ within 1 kcal mol^{-1} (overestimate) for **1**, **3** and **29a**, and within 2 kcal mol^{-1} (underestimate) for **4b**. We also calculated the barriers to VCPR for diastereoisomeric **27a** and **27b** using the M05-2X/6-31+G* method, obtaining values of $\Delta G^{\ddagger}$ (at 298 K) of 26.2 and 29.9 kcal mol^{-1} respectively, compared to the (approximate) experimental values (at 298 K) of 27.8 and 29.9 kcal mol^{-1}, respectively.

The UM06-2X functional[70] overestimated the rearrangement barrier for **1**, **3** and **29a** by 4 kcal mol^{-1} or more, performing better for more highly fluorinated **4b**. Smart's highly fluorinated **4b** involves a different type of radical terminus from the other three systems; in **4b**, the inverting radical centre is difluorinated and pyramidal, whereas it is a trigonal centre (methylene, -CH_2 in **TS1**, **TS3**) or a trigonal (benzylic methine, -CHPh in **TS29a**) in the other systems. While there is no a priori reason why the level of theory used should deal with the highly fluorinated system less well, there is a step change in structure between Smart's system and the other members of the test set.

While the UM05-2X/6-31+G* method gave the closest agreement between prediction and experimental values for this small test set, the consistency of performance of the UB3LYP/6-31G* method suggested that it would be worthwhile to assess its ability to rationalise and predict the reaction stereospecificity. Both methods were applied and the different free energies obtained are identified by a suffix in $G_{UM05\text{-}2X}$ or G_{UB3LYP}.

The important competing pathways are the *cis*/*trans* cyclopropane stereoisomerisation and the [3,3]-rearrangement of the *cis*-cyclopropane. We therefore set out to establish a minimal pathway for the former, because the full PES accessible from VCP **1** and mapped by Houk and co-workers was quite complex.[65] IRCs were computed by Houk and co-workers from *s-trans* vinylcyclopropane for the facile stereomutation; Houk identified intermediate **30** and transition state **31**, connected by rotation around a C–C σ-bond (which cost ca. 15 kcal mol^{-1} from single-point calculations) as accessible from **1** (Scheme 10).

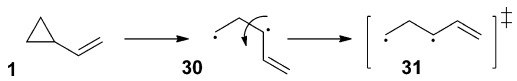

Scheme 10. Diradical species implicated in cyclopropane stereoisomerisation.

We checked that an IRC lead to intermediates of this type by stretching the ring bond distal to the CF_2 centre (using AM1 and the energy profile algorithm in Spartan'10). We then built a minimal set of triplet diradicals corresponding to the full VCPR systems.

Stretching the distal ring bond in the *s-trans* conformer of **TS29a** led to *transoid* triplet diradical **32a** (Scheme 11); the locations of the C-4 and C-6 C–H bonds echo their relative orientations in the VCP.

The interconversion was predicted to be more facile than VCPR by both methods (Table 5), consistent with the experimental findings, with the UM05-2X/6-31+G* method predicting a significantly higher barrier.

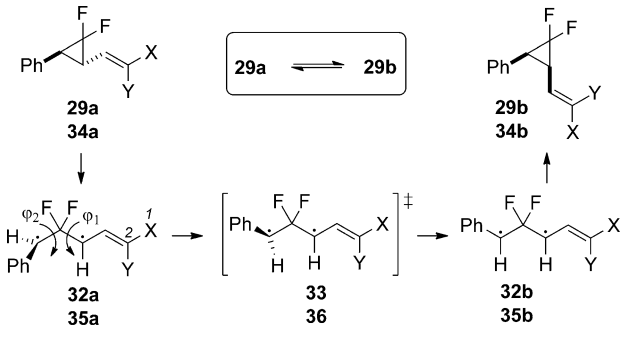

E-series **29a, 29b, 32a**, **33**, **32b**; X = CO_2Me, Y = H;
Z-series **34a, 34b, 35a**, **36**, **35b**; X = H, Y = CO_2Me.

Scheme 11. Cyclopropane *trans*/*cis* stereoisomerisation via triplets.

Table 5. Relative free energies (*G*, gas phase, 298 K, kcal mol^{-1}) for cyclopropanes (**29**, **34**), ring-opened triplets (**32**, **35**) and triplet interconversion transition states (**33**, **36**).

Species	$(G_{UM05\text{-}2X})_{rel}$	$(G_{UB3LYP})_{rel}$	Species	$(G_{UM05\text{-}2X})_{rel}$	$(G_{UB3LYP})_{rel}$
29a	0.0	0.0	**34a**	0.0	0.0
32a	23.4	19.4	**35a**	24.1	19.8
33	24.5	22.0	**36**	27.7	23.0
32b	24.1	20.5	**35b**	26.6	20.1
29b	0.5	0.6	**34b**	0.0	0.8

Conversion to *cisoid* triplet **32b** could be achieved either by rotation around C-4/C-5 (dihedral φ_1) or C-5/C-6 (dihedral φ_2) bonds; carbons C-1, C-2, C-3 and C-4 stay mutually coplanar to preserve radical stabilisation via conjugation (which explains why alkenoate *E*/*Z* stereoisomerisation was never observed). We found triplets **32a** and **32b** as minima, and connecting transition state **33** related by rotation around φ_2 (Figure 7).

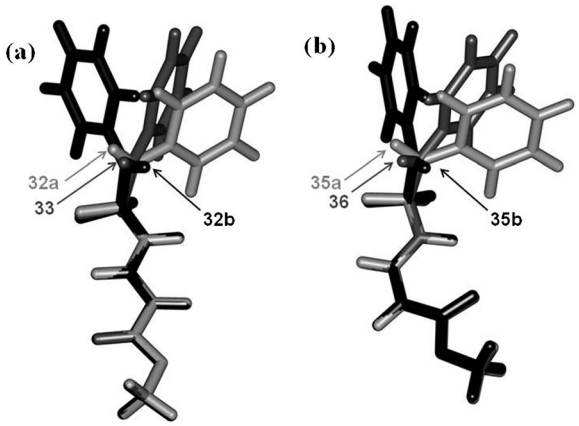

Figure 7. Triplet diradical structures which interconnect *cis*- and *trans*-cyclopropane structures for a) *E*-alkenoate and b) *Z*-alkenoate series.

The *Z*-cyclopropane **34a** and **34b** could be interconverted by rotation around φ_2 via triplets **35a** and **35b**, passing through transition state **36** (see the Supporting Information for details) at similar cost.

The VCPR transition state develops from precursors in the *gauche* conformation; isotopic labelling has been used extensively in the literature to show that while the *si* pathway is the major one, it competes with others (*ar*, *ai* and *sr*) to varying degrees depending on the number and site of isotopic labels.[65] The introduction of much bigger groups could lead to one pathway being favoured more decisively; this was our expectation given the formation of a single *trans*-cyclopentene product.

The most logical progression of **29a** would be through **TS29a** or **TS29b** (Scheme 12) which differ only in the ester conformation; inversion in the migrating benzylic centre means that by the time the transition state is reached, the phenyl group has swung into the correct orientation for the formation of the *trans*-cyclopentene product **37. TS29a** ($\Delta G^{\ddagger}_{UM05\text{-}2X}$ 29.8 kcal mol^{-1} from **29a** in the the *s-trans* confor-

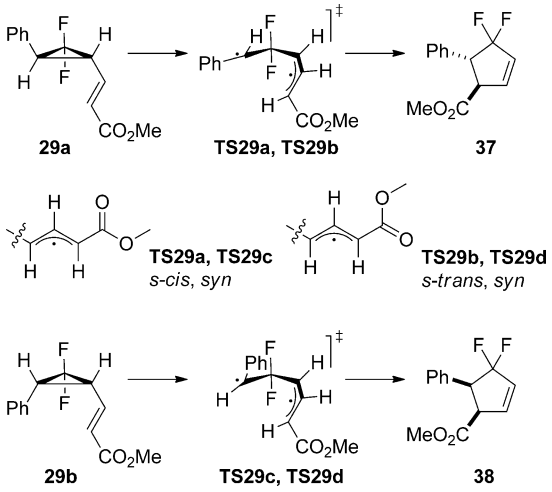

Scheme 12. Diastereoisomeric VCPR transition states.

mation, referring to the orientation of cyclopropane and alkene) has the alkenoate in the *s-cis syn* conformation, which is the favoured orientation for simpler systems like methyl acrylate;[79] **TS29b** has the ester *s-trans syn* at a cost of an additional 1 kcal mol^{-1} at the barrier ($\Delta G^{\ddagger}_{UM05\text{-}2X}$ 30.8 kcal mol^{-1}).[80]

Because the reactions appeared so stereospecific from the NMR experiments, we built and investigated a further six *si* transition states; the variables were the alkene configuration (*E*- or *Z*-) and the orientations of the Ph and -CO_2Me groups.

The formation of *cis*-cyclopentene product **38** from these competitive transition states would be anticipated strongly, contrary to the experimental findings. Simulation of the reaction profile (see the Supporting Information) predicts that *cis*-cyclopentene would make up to 20% of the product mixture when the rates of VCPR are the same for both cyclopropane diastereoisomers. An alternative explanation for the completely stereoselective VCPR would involve product epimerisation; there is a modest calculated driving force ($\Delta\Delta G_{UM05\text{-}2X}$) for the *cis*/*trans* isomerisation of **38** to **37** of only 1.4 kcal mol^{-1} (or K= 6.3 at 373 K) which is inadequate to explain the outcome. In contrast, the UB3LYP method predicted a kinetically *trans*-selective VCPR, with bigger free energy differences between the diastereoisomeric transition states. The value of $\Delta\Delta G^{\ddagger}_{UB3LYP}$ of 2.3 kcal mol^{-1} corresponds to a kinetic ratio of **37**:**38** of $>$20:1, which would predict that *cis*-product **38** would not be detected in product mixtures by ^{19}F NMR spectroscopy. Table 6 summarises the outcomes using the two methods.

Table 6. Barriers ($\Delta G^{\ddagger}$, gas phase, 298 K, kcal mol^{-1}) for VCPR from diastereoisomeric transition states.

TS	$\Delta G^{\ddagger}_{UM05\text{-}2X}$	$\Delta G^{\ddagger}_{UB3LYP}$
TS29a	29.8	25.9
TS29b	30.8	26.6
TS29c	30.1	28.2
TS29d	30.8	28.9
TS39d	34.7	32.8

The other four transition states from the set started from the *Z*-alkenoate; only one (**TS39d**) of the four optimised to a geometry recognisable as a VCPR transition state, 34.7 kcal mol^{-1} above **34a** ($\Delta G^{\ddagger}_{UM05\text{-}2X}$), so there is only one pair of diastereoisomeric structures related by opposite alkene configurations. The additional cost of access to this structure may arise from close approach (2.65 Å) between the benzylic proton and the alkenoate carbonyl carbon. When the ester was posed in the alternate *s-trans syn* conformation, a different (6,5 bicyclic) ring closure with a very high barrier ($\Delta G^{\ddagger}_{UM05\text{-}2X}$ = 55.2 kcal mol^{-1}) was indicated.

The two alternate transition structures failed to optimise to structures which corresponded to VCPR. Figure 8 shows the

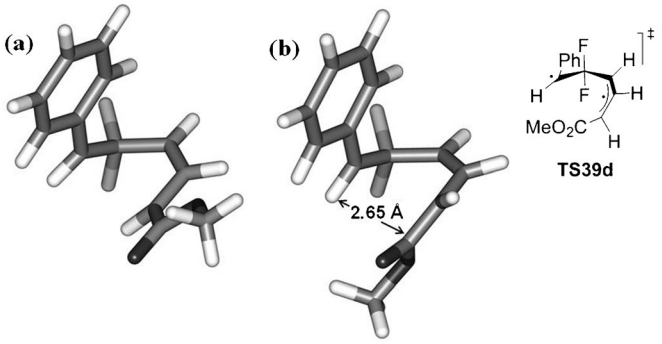

Figure 8. Alkene diastereoisomeric transition structures, both with *s-trans*, *syn* alkenoate conformation: a) **TS29d** from *E*-alkenoate series ($\Delta G^{\ddagger}_{UM05\text{-}2X}$ = 30.8 kcal mol^{-1} and $\Delta G^{\ddagger}_{UB3LYP}$ = 28.9 kcal mol^{-1}); b) **TS39d** from *Z*-alkenoate series ($\Delta G^{\ddagger}_{UM05\text{-}2X}$ = 34.7 kcal mol^{-1} and $\Delta G^{\ddagger}_{UB3LYP}$ = 32.8 kcal mol^{-1}) showing the H···C close contact.

pair of transition structures (**TS29d** and **TS39d**) which differ only in the alkene configuration and thus lead to *cis* and *trans* products respectively. These transition structures lie 30.8 and 34.7 kcal mol^{-1}, respectively, above their precursors from the UM05-2X data, and 28.9 and 32.8 kcal mol^{-1}, respectively, above their precursors from UB3LYP, showing the higher cost (3.9 kcal mol^{-1} with both methods) of rearrangement from the *Z*-series.

The concerted [3,3]-rearrangement pathway was examined for the formation of the benzocycloheptadienes from the *cis*-cyclopropanes; from M05-2X calculations, the *cis-E* TS **40** lies 27.7 kcal mol^{-1} above precursor **29b**; cis-*Z* TS **41** has a higher barrier at 34.7 kcal mol^{-1} above the *cis-Z* precursor **34b** (Figure 9). The corresponding values from the B3LYP calculations were 27.8 and 32.9 kcal mol^{-1}, respectively.

There is an eclipsing interaction between a C–H bond and a C–C bond in **41**, which results in the higher barrier. Once again, the alkene configuration has a decisive effect on reactivity, consistent with the experimental observations in which the *Z*-species only reacted at significantly higher temperature.

The immediate product **42** has lost aromaticity and therefore lies above precursor **29b**; ($(G_{M05\text{-}2X})_{rel}$ = 9.3 kcal mol^{-1}, ($G_{B3LYP})_{rel}$ = 14.5 kcal mol^{-1}) loss of HF leads to **43a-c**. Both sets of calculations identified thermodynamic product **43b** correctly

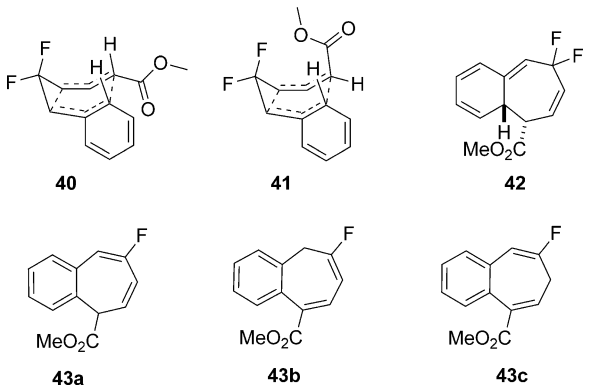

Figure 9. Initial (**42**) and final (**43a**–**c**) [3,3]-rearrangement products and transition states (**40**, **41**) from *cis*-cyclopropanes.

(for **43a** $(G_{M05\text{-}2X})_{rel} = -19.0$ kcal mol^{-1}, $(G_{B3LYP})_{rel} = -9.4$ kcal mol^{-1}; for **43b** $(G_{M05\text{-}2X})_{rel} = -22.8$ kcal mol^{-1}, $(G_{B3LYP})_{rel} = -14.5$ kcal mol^{-1}; for **43 c** $(G_{M05\text{-}2X})_{rel} = -19.6$ kcal mol^{-1}, $(G_{B3LYP})_{rel} = -11.1$ kcal mol^{-1}). Overall, the VCPR reactions to **37** ($(G_{M05\text{-}2X})_{rel} = -26.8$ kcal mol^{-1}, $(G_{B3LYP})_{rel} = -21.1$ kcal mol^{-1}) and **38** ($(G_{M05\text{-}2X})_{rel} = -26.8$ kcal mol^{-1}, $(G_{B3LYP})_{rel} = -18.4$ kcal mol^{-1}) were strongly exergonic from precursors **29a** and **29b**, respectively.

Our initial interest in carrying out electronic structure calculations based on this set of reactions arose from a wish to order the reactivities of the competing pathways successfully; *cis*/*trans* cyclopropane stereoisomerisation, stereoselective *trans*-cyclopentene formation by VCPR, [3,3]-rearrangement versus VCPR and the low reactivity of *Z*-alkenoates versus the *E*-diastereoisomers all required explanation. The two computational methods selected deal with these questions differently, as summarised in Table 7.

Of the two methods used, UB3LYP/6-31G* (with B3LYP/6-31G* for the closed shell systems) orders the pathways correctly by reactivity, predicts the stereoselectivity of the VCPR in agreement with experiment and rationalises the effect of alkene configuration on VCPR and [3,3]-rearrangement rates. While the UM05-2X/6-31 + G* method provided the highest accuracy at lowest cost for the VCPR test set, the agreement between predicted and experimental reactivity order suggests strongly that the older UB3LYP/6-31G* method may prove most effective for triage of new synthetic reactions.

Table 7. Barriers ($\Delta G^{\ddagger}$) and differences ($\Delta\Delta G^{\ddagger}$) between barriers (gas phase, 298 K, kcal mol^{-1}) relating to selectivities between isomerisation, VCPR and [3,3]-rearrangement pathways.

Pathway/process	M05-2X	B3LYP
cyclopropane isomerisation **29a**/**29b**, $\Delta G^{\ddagger}$	24.5	22.0
cyclopropane isomerisation **34a**/**34b**, $\Delta G^{\ddagger}$	27.7	23.0
lowest cost VCPR, $\Delta G^{\ddagger}$	29.8	25.9
lowest cost [3,3]-rearrangement from **29b**, $\Delta G^{\ddagger}$	27.7	27.8
selectivity for formation of kinetic *trans*-product, **37** versus **38**, $\Delta\Delta G^{\ddagger}$	0.3	2.3
E versus *Z* selectivity for VCPR, $\Delta\Delta G^{\ddagger}$	5.5	3.9
E versus *Z* selectivity for [3,3]-rearrangement, **40** versus **41**, $\Delta\Delta G^{\ddagger}$	7.0	5.1

Conclusion

We have developed a synthetic route which allows access to all four isomers of ethyl 3-(1′(2′2′-difluoro-3′-phenyl)cyclopropyl) propenoate from commercially available precursors using Dolbier's robust and effective difluorocarbene transfer reagent MDFA. Cyclopropane stereoisomerisation was facile at 100 °C in toluene and this process was monitored with VCPR by ^{19}F NMR spectroscopy. The *trans-E* isomer (**18a**) was synthetically easiest to access and rearranged to difluorocyclopentene **23** in close to quantitative yield. The overall yield of **23** over four steps from cinnamyl acetate was 70%. Our results show clearly that the alkene configuration controls which rearrangement pathway is followed; *E*-isomers underwent VCPR, whereas [3,3]-rearrangement was more favourable for *Z*-isomers. While the UM05-2X/6-31 + G* method provided the highest accuracy at lowest cost for the VCPR test set, the agreement between predicted and experimental reactivity order suggests strongly that the older UB3LYP/6-31G* method may prove most effective for triage of new synthetic reactions.

Work is currently underway to design and access more complex difluorocyclopentenes using a combination of computational triage and synthetic chemistry.

Experimental Section

Screening of other difluorocarbene sources, experimental procedures and spectral data for all new compounds, selected intermediates and crude products, kinetic raw data, simulation data and Arrhenius plot, summary of computational energies and Cartesian coordinates (B3LYP/6–31G* and M05–2X/6–31 + G* optimised structures) are provided in Supporting Information.

General experimental: NMR spectra were recorded on Bruker DPX-400 and AV-500 spectrometers. ^{1}H, ^{19}F and ^{13}C NMR spectra were recorded using the deuterated solvent as the lock and the residual solvent as the internal reference. The multiplicities of the spectroscopic data are presented in the following manner: s = singlet, d = doublet, dd = double doublet, ddd = doublet of doublet doublets, dddd = doublet of doublet of doublet of doublets; dt = doublet of triplets, ddt = doublet of double triplets, dtd = doublet of triple doublets, t = triplet, tdd = triplet of double doublets, q = quartet, m = multiplet and br. = broad. Unless stated otherwise, all couplings refer to ^{3}J homocouplings. All ^{1}H spectra are fully assigned. IR spectra were recorded on an ATR IR spectrometer. GC/MS spectra were obtained on an instrument fitted with a DB5-type column (30 m × 0.25 μm) running a 40–320 °C temperature program, ramp rate 20 °C min^{-1} with helium carrier gas flow at 1 cm^{3} min^{-1}. Chemical ionisation (CI) (methane) mass spectra were recorded on an Agilent Technologies 5975C mass spectrometer. HRMS measurements were obtained from a Thermofisher LTQ Orbitrap XL (APCI) or Finnigan MAT 95 XP (EI) spectrometers (EPSRC National Mass Spectrometry Service Centre, Swansea). Thin layer chromatography was performed on pre-coated aluminium-backed silica gel plates (E. Merck A.G., Darmstadt, Germany. Silica gel 60 F254, thickness 0.2 mm). Visualisation was achieved by using potassium permanganate or UV detection at 254 nm. Column chromatography was performed on silica gel (Zeochem, Zeoprep 60

HYD, 40–63 μm) using a Büchi Sepacore system. Hexane was distilled before chromatography. All glassware used in the synthesis of methyl(trifluoromethyl)dioxirane was washed with an aqueous solution of ethylenediaminetetraacetic acid (0.1 M) to remove trace metals and then oven dried (150 °C) before use. Diglyme was distilled from CaH_2 (60 °C/23 mbar) and stored under nitrogen over CaH_2.Trimethylsilyl chloride was distilled from CaH_2 (60 °C/430 mbar) and stored under nitrogen over CaH_2 in the refrigerator. Methyl 2,2-difluoro-2-(fluorosulfonyl)acetate (MDFA) was purchased from Fluorochem and stored under a headspace of nitrogen. Potassium iodide (Sigma Aldrich) was dried in the oven (150 °C) before use. DCM (for oxidation/Wittig reactions) was dried using a PureSolv system from Innovative Technology, Inc. All other chemicals were purchased from Sigma Aldrich, Apollo Scientific, Alfa Aesar, or Fluorochem and used as received.

Preparation of 10: An oven-dried two-necked round-bottomed flask containing potassium iodide (3.68 g, 22.2 mmol) was sealed with a SubaSeal, and the salt was stirred and lightly flame dried under an atmosphere of argon. A low boiling point water condenser with a gas outlet connected to an argon/vacuum manifold was attached and the reaction flask and the atmosphere were purged three times. Cinnamyl acetate **9** (1.34 mL, 8.0 mmol) followed by diglyme (1.3 mL) were added and the yellow suspension was heated to 120 °C. Once the reaction temperature had been reached, TMSCl (2.6 mL, 19.7 mmol) and MDFA (2.6 mL, 19.7 mmol) were added dropwise in that order. After 5 h, the reaction mixture had evaporated to dryness and a further portion of diglyme (1.3 mL) was added. The mixture was stirred for a further 19 h (total reaction time of 24 h). The resulting brown solution was cooled to room temperature and the reaction mixture was quenched with aqueous NaCl (10 mL) and diethyl ether (10 mL) added. The organic layer was separated and the aqueous layer was extracted with diethyl ether (2×10 mL). The original organic layer and the extracts were combined, dried ($MgSO_4$) and concentrated under reduced pressure to remove volatiles. The ^{1}H NMR spectrum of the resulting brown oil confirmed full conversion. Column chromatography on silica gel (2:23 diethyl ether/hexane) afforded acetate **10** as a pale yellow oil (1.7 g, 94%). R_f = 0.26 (1:9 diethyl ether/hexane); ^{1}H NMR (400 MHz, $CDCl_3$): δ = 7.36–7.29 (m, Ar*H*, 3H), 7.23–7.21 (br. d, J = 7.9 Hz, Ar*H*, 2H), 4.38 (br. ddd, J = 11.9, ^4J = 2.5 and 1.0 Hz, CH_aH$_b$OAc, 1H), 4.25 (br. dd, J = 7.8, ^4J = 1.6 Hz, CH$_a$$H_b$OAc, 1H), 2.68 (dd, J_{H-F} = 14.5 Hz, J = 7.8 Hz, PhC*H*, 1H), 2.33–2.24 (m, C(*H*)CH$_2$OAc, 1H), 2.10 ppm (s, OC(O)CH_3, 3H); ^{13}C NMR (100 MHz, $CDCl_3$): δ = 170.9, 132.7, 128.6, 128.2, 127.5, 113.1 (t, $^1J_{C-F}$ = 289.4 Hz), 60.9 (d, J_{C-F} = 5.6 Hz), 32.0 (t, $^2J_{C-F}$ = 11.2 Hz), 28.0 (t, $^2J_{C-F}$ = 10.3 Hz), 20.8 ppm; ^{19}F NMR (376 MHz, $CDCl_3$): δ = −135.4 (dd, ^2J = 157.8 Hz, J_{F-H} = 14.5 Hz, CF_aF$_b$, 1 F), −137.3 ppm (dd, ^2J = 158.6 Hz, J_{F-H} = 14.0 Hz, CF$_a$$F_b$, 1 F); $\tilde{\nu}$/(film) = 2386, 2354, 1737, 1225, 1017, 999, 972, 696 cm^{-1}; MS (CI): *m/z* (%): 167 (55) [*M*−OAc]$^+$, 147 (100); HRMS (EI): calcd for $C_{12}H_{12}F_2O_2$, 226.0800 [*M*], found 226.0861; t_R (GC) = 11.37 min. The data was in agreement with that reported by Kobayashi and co-workers but no ^{13}C NMR data was reported.[81,82]

Preparation of 11: A solution of potassium carbonate (443 mg, 3.2 mmol) in H_2O (2 mL) was added to a solution of acetate **10** (718.7 mg, 3.2 mmol) in MeOH (60 mL, 0.05 M) and the mixture was heated to 60 °C for 1 hour. Full conversion was confirmed by TLC. The reaction mixture was concentrated under reduced pressure and the resulting suspension taken up in MeOH (5 mL) and evaporated onto Celite (6.4 g). The solid was transferred onto a sinter funnel and the product was eluted with diethyl ether (60 mL). The filtrate was concentrated under reduced pressure to afford alcohol **11** as a colourless oil (583.5 mg, 99%). Compound was of a high analytical standard that no purification was required (corresponding NMR data on pages S22–S25 in the Supporting Information). R_f = 0.16 (1:4 diethyl ether/hexane); ^{1}H NMR (400 MHz, $CDCl_3$): δ = 7.38–7.30 (m, Ar*H*, 3H), 7.27–7.25 (m, Ar*H*, 2H), 4.01–3.86 (br. m, CH_2OH, 2H), 2.65 (ddd, J_{H-F} = 13.5, J = 7.6, ^4J = 1.4 Hz, PhC*H*, 1H), 2.23 (m, C*H*CH$_2$OH, 1H), 1.72 ppm (t, J = 5.9 Hz, CH$_2$O*H*, 1H); ^{13}C NMR (100 MHz, $CDCl_3$): δ = 132.5, 128.1, 127.6, 126.8, 113.9 (t, $^1J_{C-F}$ = 289.1 Hz), 59.3 (d, J_{C-F} = 5.5 Hz), 31.0 (t, $^2J_{C-F}$ = 10.7 Hz), 30.7 ppm (t, $^2J_{C-F}$ = 9.6 Hz); ^{19}F NMR (376 MHz, $CDCl_3$): δ = −136.2 (dd, ^2J = 158.1 Hz, J_{F-H} = 14.0 Hz, 1 F), −136.9 ppm (dd, ^2J = 157.6 Hz, J_{F-H} = 13.5 Hz, 1 F); $\tilde{\nu}$/(film) = 3321 (br.), 1500, 1474, 1447, 1269, 1013, 698 cm^{-1}; MS (CI): *m/z* (%): 185 (4) [*M*+H]$^+$, 167 (21) [*M*−OH], 147 (100) [(*M*+H)−F$_2$]$^+$, HRMS (APCI): calcd for $C_{10}H_{10}F_2O$, 184.0694 [*M*−H]$^+$, found 184.0688; t_R (GC) = 10.56 min. Alcohol **11** has been reported in the literature but no characterisation data was reported.[82] The compound was also reported recently by Itoh and co-workers[55] though the material isolated was of lower quality than that used in our study.

Preparation of 18a/18b: Bis(acetoxy)iodobenzene (1.35 g, 4.23 mmol) was added to a solution of alcohol **11** (678 mg, 3.68 mmol) and TEMPO (54 mg, 0.368 mmol) in anhydrous DCM (15 mL) and the reaction mixture was stirred at room temperature under nitrogen for 6 h. The ^{1}H NMR spectrum showed complete conversion to the corresponding aldehyde. (Ethoxycarbonylmethylene)triphenylphosphorane (1.64 g, 4.7 mmol) was then added to the reaction mixture and stirred for 2 h until the ^{1}H or ^{19}F NMR spectrum showed complete conversion. The resulting orange solution was concentrated under reduced pressure and column chromatography on silica gel (1:19 diethyl ether in hexane) afforded **18a** (728 mg, 78%) and **18b** (43 mg, 5%). Data for **18a**: R_f = 0.30 (1:9 diethyl ether/hexane); ^{1}H NMR (500 MHz, $CDCl_3$): δ = 7.40–7.31 (m, Ar*H*, 3H), 7.27–7.25 (m, Ar*H*, 2H), 6.79 (ddt, J = 15.6, 9.5 Hz, $^4J_{H-F}$ = 1.5 Hz, *H*C=CHCO$_2$Et, 1H), 6.09 (d, J = 15.6 Hz, HC=C*H*CO$_2$Et, 1H), 4.25 (q, J = 7.2 Hz, CO$_2$CH_2CH$_3$, 2H), 2.91 (dd, J_{H-F} = 14.7, J = 7.3 Hz, PhC*H*, 1H), 2.66–2.60 (ddd, J_{H-F} = 13.4 J = 9.5, 7.3 Hz, C*H*CH=CH, 1H), 1.33 ppm (t, J = 7.2 Hz, CO$_2$CH$_2$CH_3, 3H); ^{13}C NMR (100 MHz, $CDCl_3$): δ = 165.0, 139.8, 131.8, 128.2, 127.4, 127.2, 123.2, 112.9 (t, $^1J_{C-F}$ = 292.6 Hz), 59.9, 35.4 (t, $^2J_{C-F}$ = 9.8 Hz) 33.1 (t, $^2J_{C-F}$ = 12.7 Hz), 13.7 ppm; ^{19}F NMR (376 MHz, $CDCl_3$): δ = 130.6 (dd, ^2J = 157.4 Hz, J_{F-H} = 14.7 Hz, 1 F), - 135.6 ppm (dd, ^2J = 156.6 Hz, J_{F-H} = 13.4 Hz, 1 F); $\tilde{\nu}$/(film) = 2359, 2342, 1715, 1281 cm^{-1}; MS (CI): *m/z* (%): 233 (100) [*M*−F], 187 (44), 159 (26); HRMS (APCI): calcd for $C_{14}H_{15}F_2O_2$, 253.1035 [*M*+H]$^+$, found 253.1034; t_R (GC) = 12.13 min. Data for **18b**: R_f = 0.43 (1:9 ethyl acetate/hexane); ^{1}H NMR (400 MHz $CDCl_3$): δ = 7.40–7.29 (m, Ar*H*, 5H), 6.06–5.99 (m, *H*C=C*H*CO$_2$Et, 2H), 4.234 (q, J = 7.2 Hz, OCH_aH$_b$CH$_3$, 1H), 4.225 (q, J = 7.2 *Hz*, OCH$_a$$H_bCH_3$, 1H), 4.18–4.10 (m, *H*CCH=CHCO$_2$Et, 1H), 2.84 (dd, J_{H-F} = 14.8 Hz, J = 7.1 Hz, C*H*Ph, 1H), 1.32 ppm (t, J = 7.2 Hz, CH_3, 3H); ^{13}C NMR (100 MHz, $CDCl_3$): δ = 165.7, 140.1 (d, J_{C-F} = 6.3 Hz), 131.7, 128.1, 127.7, 127.1, 121.3, 113.5 (t, $^1J_{C-F}$ = 291.1 Hz), 59.8, 36.2 (dd, $^2J_{C-F}$ = 11.8, 9.1 Hz), 30.1 (dd, $^2J_{C-F}$ = 13.6, 9.9 Hz), 13.7 ppm; ^{19}F NMR (376 MHz, $CDCl_3$): δ = −132.3 (dd, ^2J = 154.3 Hz J_{F-H} = 14.8 Hz, 1 F), −136.2 ppm (dd, ^2J = 154.6 Hz J_{F-H} = 13.7 Hz, 1 F); $\tilde{\nu}$/(film) = 2359, 2342, 1715, 1194, 1018, 806 cm^{-1}; MS (CI): *m/z* (%): 281 (4) [*M*+C$_2$H$_5$]$^+$, 253 (70) [*M*+H]$^+$, 233 (35) [*M*−F], 225 (36), 205 (60) [(*M*+H)−(F+Et)]$^+$, 187 (100), 179 (30) [*M*−CO$_2$Et], 169 (18) [*M*−F$_2$+OEt], 159 (45), 141 (28) [*M*−F$_2$+CO$_2$Et]; HRMS (APCI): calcd for $C_{14}H_{15}F_2O_2$, 253.1035 [*M*+H]$^+$, found 253.1035; t_R (GC) = 12.36 min.

Preparation of 23: A solution of **18a** (104 mg, 0.4 mmol) in toluene (0.5 mL) was heated to 100 °C in a sealed microwave vial for 17 h in a DrySyn block. After cooling and venting the vial, fluorine NMR confirmed complete conversion. The reaction mixture was transferred to a round bottom flask using DCM (5 mL) and concen-

trated under reduced pressure to afford difluorocyclopentene **23** (102 mg, 99%) as a pale yellow oil. $R_f = 0.34$ (1:4 diethyl ether/hexane); ^{1}H NMR (400 MHz, $CDCl_3$): $\delta = 7.41$–7.33 (m, Ar*H*, 5H), 6.50 (dt, $J = 6.0$, $^4J_{H-F} = 1.6$ Hz, =*CH*CO_2Et, 1H), 6.09 (dd, $J = 6.0$, $J_{H-F} = 2.5$ Hz, =*CH*CF_2, 1H), 4.18 (q, $J = 7.1$ Hz, O$CH_2$$CH_3$, 2H), 4.04–3.92 (m, *CH*CO_2Et, *CH*Ph, 2H), 1.26 ppm (t, $J = 7.1$ Hz, O$CH_2$$CH_3$, 3H); ^{13}C NMR (400 MHz, $CDCl_3$): $\delta = 170.3$ (d, $^4J_{C-F} = 4.8$ Hz), 138.6 (t, $J_{C-F} = 10.4$ Hz), 133.8, 129.3 (t, $^1J_{C-F} = 245.7$ Hz), 128.7, 128.5 (dd, $^2J_{C-F} = 25.0$, 30.3 Hz), 128.0, 127.3, 61.0, 54.1 (d, $J_{C-F} = 6.0$ Hz), 53.2 (t, $^2J_{C-F} = 24.6$ Hz), 13.6 ppm; ^{19}F NMR (376 MHz, $CDCl_3$): $\delta = -89.3$ (ddd, $^2J = 252.8$ Hz, $J_{F-H} = 16.6$, 8.9 Hz, 1 F), -92.7 ppm (ddd, $^2J = 253.2$ Hz, $J_{F-H} = 14.2$, 5.8 Hz, 1 F); $\tilde{\nu}$/(film) = 2359, 2340, 1732, 1254, 1194, 1167, 698 cm^{-1}; MS (CI): *m/z* (%): 253 (3) $[M+H]^+$, 233 (100) $[M-F]$, 215 (8), 187 (40), 159 (33); HRMS (APCI): calcd for $C_{14}H_{15}FO_2$, 253.1035 $[M+H]^+$ found 253.1033; t_R (GC) = 12.13 min.

Computational Methodology

Structures were built in Spartan'08 or Spartan'10 and Monte Carlo conformational searching was carried out using the MMFF94 molecular mechanics method. Relatively small sets of conformers (4 typically) were obtained and geometry optimisation calculations were carried out for all members of the sets using the UB3LYP functional (invoked using the keywords MIX and SCF = UNRESTRICTED, with CONVERGE deprecated). In cases where SCF convergence was difficult, the keyword NODIIS was used. The 6–31G* basis set was used throughout and calculations were carried out in vacuo. Calculations were carried out on a Dell Precision T1500 (Intel i7 Quad Core, 2.93 GHz) with 8GB RAM, Microsoft Windows 7 OS 64-bit, or a Dell Precision T7500 (2 x Intel E5530 processors, four cores each, 2.40 GHz) with 24 GB RAM Debian GNU/Linux 5. Calculations using the M05–2X/6–31 + G* method were carried out using Gaussian09[75] on cluster hardware. Full references for Spartan can be found in the Supporting Information.

Acknowledgements

We thank GSK (Dr Vipulkumar K. Patel) and the University of Strathclyde (studentship to D. O.), the EPRSC National Mass Spectrometry Service Centre, Swansea for accurate mass measurements, and Craig Irving (NMR Technician, University of Strathclyde) for assistance with NMR kinetic experiments.

Keywords: activation parameters · density functional calculations · difluorocyclopentene · rearrangements · stereoselectivity

[1] N. Neureiter, *J. Org. Chem.* **1959**, *24*, 2044.
[2] T. Hudlicky, J. W. Reed, *Angew. Chem.* **2010**, *122*, 4982; *Angew. Chem. Int. Ed.* **2010**, *49*, 4864.
[3] Z. Goldschmidt, B. Crammer, *Chem. Soc. Rev.* **1988**, *17*, 229.
[4] J. E. Baldwin, *Chem. Rev.* **2003**, *103*, 1197.
[5] C. G. Overberger, A. E. Borchert, *J. Am. Chem. Soc.* **1960**, *82*, 4896.
[6] E. Vogel, *Angew. Chem.* **1960**, *72*, 4.
[7] R. L. Danheiser, C. Martinez-Davila, J. M. Morin, *J. Org. Chem.* **1980**, *45*, 1340.
[8] G. Zuo, J. Louie, *Angew. Chem.* **2004**, *116*, 2327; *Angew. Chem. Int. Ed.* **2004**, *43*, 2277.
[9] S. C. Wang, D. M. Troast, M. Conda-Sheridan, G. Zuo, D. LaGarde, J. Louie, D. J. Tantillo, *J. Org. Chem.* **2009**, *74*, 7822.
[10] L. Jiao, Z.-X. Yu, *J. Org. Chem.* **2013**, *78*, 6842.
[11] M. R. Willcott, V. H. Cargle, *J. Am. Chem. Soc.* **1967**, *89*, 723.
[12] M. R. Willcott, V. H. Cargle, *J. Am. Chem. Soc.* **1969**, *91*, 4310.
[13] R. J. Ellis, H. M. Frey, *J. Chem. Soc.* **1964**, 5578.
[14] C. A. Wellington, *J. Phys. Chem.* **1962**, *66*, 1671.
[15] D. K. Lewis, D. J. Charney, B. L. Kalra, A.-M. Plate, M. H. Woodard, S. J. Cianciosi, J. E. Baldwin, *J. Phys. Chem. A* **1997**, *101*, 4097.
[16] E. W. Schlag, B. S. Rabinovitch, *J. Am. Chem. Soc.* **1960**, *82*, 5996.
[17] S. W. Benson, A. N. Bose, P. Nangia, *J. Am. Chem. Soc.* **1963**, *85*, 1388.
[18] W. R. Dolbier, B. H. Al-Sader, S. F. Sellers, H. Koroniak, *J. Am. Chem. Soc.* **1981**, *103*, 2138.
[19] W. R. Roth, W. Kirmse, W. Hoffmann, H.-W. Lennartz, *Chem. Ber.* **1982**, *115*, 2508.
[20] R. A. Mitsch, E. W. Neuvar, *J. Phys. Chem.* **1966**, *70*, 546.
[21] B. E. Smart, P. J. Krusic, D. C. Roe, Z.-Y. Yang, *J. Fluorine Chem.* **2002**, *117*, 199.
[22] H. E. ONeal, S. W. Benson, *J. Phys. Chem.* **1968**, *72*, 1866.
[23] D. N. Zeiger, J. F. Liebman, *J. Mol. Struct.* **2000**, *556*, 83.
[24] W. R. Dolbier, *Acc. Chem. Res.* **1981**, *14*, 195.
[25] F. Tian, M. D. Bartberger, W. R. Dolbier, *J. Org. Chem.* **1998**, *63*, 540.
[26] S. Eusterwiemann, H. Martinez, W. R. Dolbier, *J. Org. Chem.* **2012**, *77*, 5461.
[27] J. M. Percy, *Top. Curr. Chem.* **1997**, *193*, 131.
[28] P. Erbes, W. Boland, *Helv. Chim. Acta* **1992**, *75*, 766.
[29] D. L. S. Brahms, W. P. Dailey, *Chem. Rev.* **1996**, *96*, 1585.
[30] W. R. Dolbier, M. A. Battiste, *Chem. Rev.* **2003**, *103*, 1071.
[31] M. Fedoryński, *Chem. Rev.* **2003**, *103*, 1099.
[32] R. Csuk, L. Eversmann, *Tetrahedron* **1998**, *54*, 6445.
[33] T. Itoh, K. Mitsukura, M. Furutani, *Chem. Lett.* **1998**, *27*, 903.
[34] A. Shibuya, A. Sato, T. Taguchi, *Bioorg. Med. Chem. Lett.* **1998**, *8*, 1979.
[35] D. Seyferth, S. P. Hopper, *J. Organomet. Chem.* **1971**, *26*, C62.
[36] D. Seyferth, S. P. Hopper, *J. Org. Chem.* **1972**, *37*, 4070.
[37] F. Wang, W. Zhang, J. Zhu, H. Li, K.-W. Huang, J. Hu, *Chem. Commun.* **2011**, *47*, 2411.
[38] A. K. Yudin, G. K. S. Prakash, D. Deffieux, M. Bradley, R. Bau, G. A. Olah, *J. Am. Chem. Soc.* **1997**, *119*, 1572.
[39] L. Li, F. Wang, C. Ni, J. Hu, *Angew. Chem.* **2013**, *125*, 12616; *Angew. Chem. Int. Ed.* **2013**, *52*, 12390.
[40] F. Tian, V. Kruger, O. Bautista, J.-X. Duan, A.-R. Li, W. R. Dolbier Jr, Q.-Y. Chen, *Org. Lett.* **2000**, *2*, 563.
[41] J.-M. Vatèle, *Tetrahedron Lett.* **2006**, *47*, 715.
[42] W. Adam, C. van Barneveld, D. Golsch, *Tetrahedron* **1996**, *52*, 2377.
[43] http://openflask.blogspot.co.uk/2014/01/tfdo-synthesis-procedure.html, Accessed February 2014.
[44] P. J. Gritsch, E. Stempel, T. Gaich, *Org. Lett.* **2013**, *15*, 5472.
[45] V. W. Bowry, J. Lusztyk, K. U. Ingold, *J. Am. Chem. Soc.* **1991**, *113*, 5687.
[46] M. Newcomb, C. C. Johnson, M. B. Manek, T. R. Varick, *J. Am. Chem. Soc.* **1992**, *114*, 10915.
[47] M. Newcomb, *Tetrahedron* **1993**, *49*, 1151.
[48] L. A. Buttle, W. B. Motherwell, *Tetrahedron Lett.* **1994**, *35*, 3995.
[49] F. Barth, O.-C. Yang, *Tetrahedron Lett.* **1991**, *32*, 5873.
[50] T. Morikawa, Y. Kodama, J. Uchida, M. Takano, Y. Washio, T. Taguchi, *Tetrahedron* **1992**, *48*, 8915.
[51] T. Mase, I. N. Houpis, A. Akao, I. Dorziotis, K. Emerson, T. Hoang, T. Iida, T. Itoh, K. Kamei, S. Kato, Y. Kato, M. Kawasaki, F. Lang, J. Lee, J. Lynch, P. Maligres, A. Molina, T. Nemoto, S. Okada, R. Reamer, J. Z. Song, D. Tschaen, T. Wada, D. Zewge, R. P. Volante, P. J. Reider, K. Tomimoto, *J. Org. Chem.* **2001**, *66*, 6775.
[52] P. E. Harrington, M. A. Tius, *J. Org. Chem.* **1999**, *64*, 4025.
[53] M. Bremer, P. Kirsch, M. Klasen-Memmer, K. Tarumi, *Angew. Chem.* **2013**, *125*, 9048; *Angew. Chem. Int. Ed.* **2013**, *52*, 8880.
[54] Y.-Y. Yang, W.-D. Meng, F.-L. Qing, *Org. Lett.* **2004**, *6*, 4257.
[55] D. Munemori, K. Narita, T. Nokami, T. Itoh, *Org. Lett.* **2014**, *16*, 2638.
[56] J. A. L. Miles, L. Mitchell, J. M. Percy, K. Singh, E. Uneyama, *J. Org. Chem.* **2007**, *72*, 12.
[57] S. H. Kyne, J. A. L. Miles, J. M. Percy, K. Singh, *J. Org. Chem.* **2012**, *77*, 991.
[58] T. Anderl, C. Audouard, A. Miah, J. M. Percy, G. Rinaudo, K. Singh, *Org. Biomol. Chem.* **2009**, *7*, 5200.
[59] C. Audouard, I. Barsukov, J. Fawcett, G. A. Griffith, J. M. Percy, S. Pintat, C. A. Smith, *Chem. Commun.* **2004**, 1526.
[60] J. E. Baldwin, K. A. Villarica, D. I. Freedberg, F. A. L. Anet, *J. Am. Chem. Soc.* **1994**, *116*, 10845.
[61] J. E. Baldwin, S. J. Bonacorsi, *J. Am. Chem. Soc.* **1996**, *118*, 8258.

[62] J. Mulzer, R. Huisgen, V. Arion, R. Sustmann, *Helv. Chim. Acta* **2011**, *94*, 1359.
[63] E. R. Davidson, J. J. Gajewski, *J. Am. Chem. Soc.* **1997**, *119*, 10543.
[64] K. N. Houk, M. Nendel, O. Wiest, J. W. Storer, *J. Am. Chem. Soc.* **1997**, *119*, 10545.
[65] M. Nendel, D. Sperling, O. Wiest, K. N. Houk, *J. Org. Chem.* **2000**, *65*, 3259.
[66] C. Doubleday, G. S. Li, W. L. Hase, *Phys. Chem. Chem. Phys.* **2002**, *4*, 304.
[67] A. D. Becke, *J. Chem. Phys.* **1993**, *98*, 5648.
[68] C. T. Lee, W. T. Yang, R. G. Parr, *Phys. Rev. B* **1988**, *37*, 785.
[69] Y. Zhao, N. E. Schultz, D. G. Truhlar, *J. Chem. Phys.* **2005**, *123*, 161103, **DOI:** 10.1063/1.2126975.
[70] Y. Zhao, N. E. Schultz, D. G. Truhlar, *J. Chem. Theor. Comput.* **2006**, *2*, 364.
[71] Y. Zhao, D. G. Truhlar, *Acc. Chem. Res.* **2008**, *41*, 157.
[72] Y. Zhao, D. G. Truhlar, *Theor. Chem. Acc.* **2008**, *120*, 215.
[73] J. Antony, S. Grimme, *Phys. Chem. Chem. Phys.* **2006**, *8*, 5287.
[74] S. Grimme, *J. Comput. Chem.* **2006**, *27*, 1787.
[75] Gaussian 09, Revision A.01, M. J. Frisch, G. W. Trucks, H. B. Schlegel, G. E. Scuseria, M. A. Robb, J. R. Cheeseman, G. Scalmani, V. Barone, B. Mennucci, G. A. Petersson, H. Nakatsuji, M. Caricato, X. Li, H. P. Hratchian, A. F. Izmaylov, J. Bloino, G. Zheng, J. L. Sonnenberg, M. Hada, M. Ehara, K. Toyota, R. Fukuda, J. Hasegawa, M. Ishida, T. Nakajima, Y. Honda, O. Kitao, H. Nakai, T. Vreven, J. A. Montgomery, Jr., J. E. Peralta, F. Ogliaro, M. Bearpark, J. J. Heyd, E. Brothers, K. N. Kudin, V. N. Staroverov, R. Kobayashi, J. Normand, K. Raghavachari, A. Rendell, J. C. Burant, S. S. Iyengar, J. Tomasi, M. Cossi, N. Rega, J. M. Millam, M. Klene, J. E. Knox, J. B. Cross, V. Bakken, C. Adamo, J. Jaramillo, R. Gomperts, R. E. Stratmann, O. Yazyev, A. J. Austin, R. Cammi, C. Pomelli, J. W. Ochterski, R. L. Martin, K. Morokuma, V. G. Zakrzewski, G. A. Voth, P. Salvador, J. J. Dannenberg, S. Dapprich, A. D. Daniels, Ö. Farkas, J. B. Foresman, J. V. Ortiz, J. Cioslowski, D. J. Fox, Gaussian, Inc. Wallingford CT, **2009**.
[76] Spartan'08, Wavefunction Inc., Irvine, CA, **2008**.
[77] Spartan'10, Wavefunction Inc., Irvine, CA, **2010**.
[78] H. Maskill, *The Physical Basis of Organic Chemistry*, OUP, Oxford, **1985**, Chapter 6, 242.
[79] R. J. Loncharich, T. R. Schwartz, K. N. Houk, *J. Am. Chem. Soc.* **1987**, *109*, 14.
[80] S. M. Bakalova, A. G. Santos, *J. Org. Chem.* **2004**, *69*, 8475.
[81] Y. Kobayashi, T. Taguchi, T. Morikawa, T. Takase, H. Takanashi, *J. Org. Chem.* **1982**, *47*, 3232.
[82] Y. Kobayashi, T. Taguchi, T. Morikawa, *J. Fluorine Chem.* **1982**, *21*, 60.

Received: May 29, 2014
Published online on ■■ ▮▮, 0000

FULL PAPER

Run rings around fluorine: A difluorinated cyclopentene was accessed in high yields (70% over 4 steps) from commercial starting materials using the thermal vinyl cyclopropane rearrangement (VCPR). Alongside a relatively mild reaction temperature (100 °C), in situ cyclopropane stereomutation, a competing [3,3]-rearrangement pathway and a sharp and unexpected dependence on alkene configuration were all detected. Kinetic and electronic structure calculations were used to evaluate and rationalise these observations.

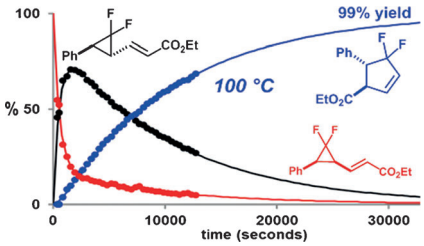

Rearrangements

D. Orr, J. M. Percy, T. Tuttle, A. R. Kennedy, Z. A. Harrison*

■■ – ■■

Evaluating the Thermal Vinylcyclopropane Rearrangement (VCPR) as a Practical Method for the Synthesis of Difluorinated Cyclopentenes: Experimental and Computational Studies of Rearrangement Stereospecificity